

Bell-state preparation for fullerene based electron spins in distant peapod nanotubes

W. L. Yang,^{1,2} H. Wei,^{1,2} X. L. Zhang,³ M. Feng^{1*}

¹*State Key Laboratory of Magnetic Resonance and Atomic and Molecular Physics, Wuhan Institute of Physics and Mathematics, Chinese Academy of Sciences, Wuhan 430071, China*

²*Graduate School of the Chinese Academy of Sciences, Beijing 100049, China and*

³*Center for Modern Physics and Department of Physics, Chongqing University, Chongqing 400044, China*

We propose a potentially practical scheme, in combination with the Bell-state analyzer [Zhang *et al.*, Phys. Rev. A **73**, 014301 (2006)], to generate Bell states for two electron spins confined, respectively, in two distant C_{60} fullerenes. To this end, we consider the endohedral fullerenes staying in single walled carbon nanotubes (*SWCNTs*) and employ auxiliary mobile electrons and selective microwave pulses. The application and the experimental feasibility of our scheme are discussed.

PACS numbers: 03.67.Lx, 03.65.Ud, 73.21.-b

As a crucial resource of quantum information processing (QIP), entanglement has exhibited peculiar correlation among the degrees of freedom of single particles or the distinct parts of a composite system. Generally speaking, creation of maximally entangled states between two qubits, i.e., Einstein-Podolsky-Rosen pairs or Bell states, is the first step towards more complicated cases of entanglement. Motivated by potential applications of entanglement, there are currently great interests in finding methods to create and manipulate entangled states. Different schemes have been proposed for realizing Bell states, and the relevant experimental demonstration has been achieved in different systems [1].

One of the recently mentioned methods to generate entanglement is the use of mobile qubits. As in [2], the trapped ions hold static qubits encoded in atomic levels, and emit mobile qubits, i.e., photons, in a controllable way. As the mobile qubits have entangled with the static qubits, once we can entangle and then detect the mobile qubits, we will have the entanglement of the static qubits. In this Brief Report, we will try to move such an idea to an entanglement generation of two distant fullerene-based electron spins. Doped fullerenes, like $^{15}N@C_{60}$ or $^{31}P@C_{60}$, have been considered as excellent candidates for spin-based QIP [3, 4, 5, 6], the most attractive feature of which is the long decoherence time of the electron spin of the doped atom due to the protection from the fullerene cage. In the original QIP schemes with endohedral fullerenes, the qubits could be encoded in either electron spins [3] or nuclear spins [4] of the doped atoms. No matter which qubits are employed, the two-qubit gating is based on the dipole-dipole coupling of the electron spins between nearest-neighbor fullerenes. As a result, to entangle two distant qubits, we have to involve a lot of overhead. In this work, we consider an efficient entanglement scheme for distant fullerene-based qubits confined in single-walled carbon nanotubes (*SWCNTs*) [7, 8, 9, 10, 11]. The key idea is that we inject auxiliary single electrons with certain polarization to the potential wells in *SWCNTs*. After entangling the mobile qubits (i.e., the spins of the injected electrons) with the static qubits (i.e., the electron spins inside the fullerenes), we move the mobile qubits away and make them entangled with each other by a Bell-state analyzer [12, 13]. Then the static qubits, no matter how distant they are, will be entangled in one of the Bell states.

SWCNTs carry promises to transport information from one location to another. As shown in [8, 9], the quasi-one-dimensional nanosized structure of the *SWCNTs* offers the possibility of moving qubits in a solid-state system. Experimentally, the transport of spin-polarized electrons in a carbon nanotube has already been achieved [14] and well investigated [9, 15]. Moreover, with current technology, it is possible to trap empty or doped fullerenes in hollow *SWCNTs*, which are called fullerene peapods [16]. By using two fullerene peapods, we will demonstrate below how to entangle two distant encapsulated electron spins.

We sketch our scheme in Fig. 1, which consists of two distant $^{15}N@C_{60}@SWCNTs$ peapods encapsulating the static qubits A' and B' , respectively. Using turnstile injectors, we could have two auxiliary electrons, carrying mobile qubits A and B , injected and confined respectively in shallow potential wells in the conduction bands of the *SWCNTs*. We suppose each potential well to be shallow enough to hold only a single electron. As the electron spin of the doped atom ^{15}N is $3/2$, we encode the static qubits in the Zeeman levels $|-3/2\rangle = |\uparrow\rangle_{A'(B')}$ and $|3/2\rangle = |\downarrow\rangle_{A'(B')}$. The mobile spins A and B are defined as $|-1/2\rangle = |\uparrow\rangle_{A(B)}$ and $|1/2\rangle = |\downarrow\rangle_{A(B)}$. Let us first consider the entanglement between the mobile qubit A and the static qubit A' . Under magnetic field gradient, A and A' with different level splitting, interact by dipole-dipole coupling. Neglecting the negligible terms associated with nuclear spins, we have

*Electronic address: mangfeng@wipm.ac.cn

the Hamiltonian in units of $\hbar = 1$,

$$H = g\mu_B B_A S_z^A + g\mu_B B_{A'} S_z^{A'} + JS_z^A S_z^{A'}, \quad (1)$$

where μ_B is the Bohr magneton, g is the electron Landé g -factor, and B_i ($i = A$ and A') is the magnetic field strength experienced by qubit i . As mentioned in [4], individually addressing of qubits is available with selective microwave pulses under the magnetic field gradients generated by micropatterned wires, which can shift the resonance frequency between neighboring electron spins by several Megahertz. In Eq.(1), the magnetic dipolar coupling strength J between qubits A' and A could be expressed as $J = J_0(1 - 3\cos^2\phi)$ [3], where $J_0 = \hbar\gamma^2/|r|^3$ with γ the gyromagnetic ratio of the electron, r the distance vector between the two electron spins, and ϕ the angle between r and the magnetic field. In our case, J is estimated to be 50 MHz provided $|r| = 1.14$ nm and $\phi = 0$ as done in [4]. Furthermore, for two nearest-neighbor electron qubits distant by 1.14 nm in the magnetic field gradient $dB/dz = 4 \times 10^5$ T/m, the differences of the electron spin resonance (ESR) frequencies between neighboring encapsulated spins are about 12.7 MHz and $12.7 \times 3 \approx 38$ MHz regarding $|\pm 1/2\rangle$ and $|\pm 3/2\rangle$, respectively, and thereby the single-qubit operation is available using narrow-band ESR pulses [6].

Straightforward calculations show that the eigenenergies of Eq. (1) are

$$\begin{aligned} &2\omega_1 + 3\omega_2 + 3J/2, & 2\omega_1 + \omega_2 + J/2, & 2\omega_1 - \omega_2 - J/2, & 2\omega_1 - 3\omega_2 - 3J/2, \\ &-2\omega_1 + 3\omega_2 - 3J/2, & -2\omega_1 + \omega_2 - J/2, & -2\omega_1 - \omega_2 + J/2, & -2\omega_1 - 3\omega_2 + 3J/2, \end{aligned} \quad (2)$$

in the subspace spanned by $|\frac{1}{2}, \frac{3}{2}\rangle, |\frac{1}{2}, \frac{1}{2}\rangle, |\frac{1}{2}, -\frac{1}{2}\rangle, |\frac{1}{2}, -\frac{3}{2}\rangle, |-\frac{1}{2}, \frac{3}{2}\rangle, |-\frac{1}{2}, \frac{1}{2}\rangle, |-\frac{1}{2}, -\frac{1}{2}\rangle, |-\frac{1}{2}, -\frac{3}{2}\rangle$, where $\omega_1 =$

$$g\mu_B B_A/2, \text{ and } \omega_2 = g\mu_B B_{A'}/2, \text{ and } S_z^A \text{ and } S_z^{A'} \text{ in Eq. (1) are denoted by } S_z^A = \begin{pmatrix} 1 & 0 \\ 0 & -1 \end{pmatrix} \otimes \begin{pmatrix} 1 & 0 & 0 & 0 \\ 0 & 1 & 0 & 0 \\ 0 & 0 & 1 & 0 \\ 0 & 0 & 0 & 1 \end{pmatrix},$$

$$S_z^{A'} = \begin{pmatrix} 1 & 0 \\ 0 & 1 \end{pmatrix} \otimes \frac{1}{2} \begin{pmatrix} 3 & 0 & 0 & 0 \\ 0 & 1 & 0 & 0 \\ 0 & 0 & -1 & 0 \\ 0 & 0 & 0 & -3 \end{pmatrix}. \text{ As depicted in Fig. 2, the splitting of a spin state is heavily dependent on another}$$

coupled spin state. So some of the degeneracy are released. As a result, a $\pi/2$ ESR pulse with the frequency $2\omega_2 + J$ flip only the target state of the static qubit A' (i.e., $|\uparrow\rangle_{A'} \rightleftharpoons |\downarrow\rangle_{A'}$) in the case of the control state of the mobile qubit A being $|1/2\rangle_A$ [6]. This is a nontrivial two-qubit gate $CNOT_{AA'}$. Similarly, we can also construct another indispensable two-qubit gates $CNOT_{BB'}$ to entangle the mobile and static qubits.

Suppose that the mobile spin is initially prepared in a superposition state $(|\uparrow\rangle_{A(B)} + |\downarrow\rangle_{A(B)})/\sqrt{2}$, and the state of the static qubit is $|\downarrow\rangle_{A'(B')}$. From the initial state $|\Psi_0\rangle = (|\uparrow\rangle_A |\downarrow\rangle_{A'} + |\downarrow\rangle_A |\downarrow\rangle_{A'}) \otimes (|\uparrow\rangle_B |\downarrow\rangle_{B'} + |\downarrow\rangle_B |\downarrow\rangle_{B'})/2$, the gating $CNOT_{AA'}$ and $CNOT_{BB'}$ lead to

$$|\Psi_0'\rangle = \frac{1}{2}(|\uparrow\rangle_A |\downarrow\rangle_{A'} + |\downarrow\rangle_A |\uparrow\rangle_{A'}) \otimes (|\uparrow\rangle_B |\downarrow\rangle_{B'} + |\downarrow\rangle_B |\uparrow\rangle_{B'}). \quad (3)$$

Then the mobile qubits will be moved to the Bell-state analyzer designed in Refs. [12, 13] which makes use of the commutability between the spin and charge degrees of freedom of the electron. As plotted in Fig. 1, the two mobile qubits are sent through the analyzer from the ports a and b . By making measurement by charge detectors, as listed and explained in Table I, we could have the two mobile qubits entangled in a specific Bell state, which also implies a specific entanglement between the two static qubits.

However, there was no imperfection considered in above treatment. Recent observation [17] has shown that T_1 of the doped electron spin in *SWCNTs* is 13 μs at 300 K, and 30 μs at 5 K, respectively, which are shorter compared to the crystalline cases [18]. It was speculated that the short T_1 is due to interaction of the encapsulated electron spin with the nuclear spins in the host *SWCNTs* [17]. However, as the cage could reduce the detrimental effect from decoherence to 25% [5], we may suppose below that the mobile qubits are affected by decoherence more than the static qubits inside the cages by four times, and thereby we would only consider the decaying of the mobile qubits in our following treatment. Moreover, dephasing in our case is strongly related to the external magnetic field. As the static qubit is initially in the well polarized state, but the mobile qubit in superposition state, we will only focus our attention on the dephasing of the mobile qubits [19]. Supposing our implementation is fast enough so that no spin flip has actually happened, we consider following effective Hamiltonian $H_D^j = \theta\sigma_j^z - i\frac{\Gamma_1^j}{2}\sigma_j^+\sigma_j^-$, where σ_j^k ($k = z, +, -$) are Pauli operators for the mobile qubits with $j = A, B$, Γ_1^j is the spin-flip relaxation rate and θ is the level splitting plus the level shift due to coupling to the static qubit. From the initial state $|\Psi\rangle_0^j = (|\uparrow\rangle_j + |\downarrow\rangle_j)/\sqrt{2}$, we have

the time evolution yielding $|\Psi(t)\rangle^j = [(\cos(\theta t) - i \sin(\theta t))e^{-\frac{\Gamma_1^j}{2}t} |\uparrow\rangle_j + (\cos(\theta t) + i \sin(\theta t)) |\downarrow\rangle_j] / \sqrt{2}$. To eliminate the dephasing effect, we could employ a trick by setting the gating time to be $t_g = 2k\pi/\theta$, with k a constant determined later. So we have $|\Psi(t)\rangle^j = (e^{-\frac{\Gamma_1^j}{2}t} |\uparrow\rangle_j + |\downarrow\rangle_j) / \sqrt{2}$, which is only suffered from the spin-flip errors. To perform the $CNOT_{AA'}$ or $CNOT_{BB'}$ with this trick, we should have $k = \theta/(2\Omega_e)$ with Ω_e the Rabi frequency under the radiation of ESR pulses. As a result, the entangled state produced would not be affected by dephasing errors. To visualize the effect of spin-flip relaxation, we have plotted in Fig. 3 the fidelity of the generated Bell states $|\Psi\rangle_{A'B'}^\pm$ and $|\Phi\rangle_{A'B'}^\pm$ in the dissipative situation, which are, respectively, $F_{|\Psi\rangle_{A'B'}^\pm} = (\alpha_A + \alpha_B)^2 / (1 + \alpha_A^2)(1 + \alpha_B^2)$ and $F_{|\Phi\rangle_{A'B'}^\pm} = (1 + \alpha_A\alpha_B)^2 / (1 + \alpha_A^2)(1 + \alpha_B^2)$, with $\alpha_A = e^{-\Gamma_1^A t}$ and $\alpha_B = e^{-\Gamma_1^B t}$. Although the fidelities are generally going down with increasing relaxation rates, the Bell state $|\Phi\rangle_{A'B'}^\pm$ always keeps unit in the case of $\Gamma_1^A = \Gamma_1^B$, which could be explained by above expression $F_{|\Phi\rangle_{A'B'}^\pm}$ and is reflected in the inset of Fig. 3.

We address some remarks for experimental implementation of our scheme. First of all, in above treatment for imperfection, we have only considered the dephasing due to external magnetic field, which is avoidable by our trick. However, the intrinsic dephasing errors due to the nuclear spin of the impurity atom ^{13}C is hard to be overcome. In the absence of external magnetic field, T_2 remains about $20 \mu\text{s}$ at 5 K for both fullerene peapods and crystalline fullerenes [17]. As T_2 is shorter than T_1 , we should consider it seriously in designing our scheme. Our operations include transport of mobile qubits and logic gating. It was reported [9, 15] that the transport time of the mobile qubit with Fermi velocity 10^6 m/s could be as short as 1 picosec over a $1 \mu\text{m}$ $SWCNT$ [20], and our operation time shown above could be shorter than $0.1 \mu\text{s}$ in the case of $\Omega_e = 25 \text{ MHz}$. As a result, the influence from intrinsic dephasing is negligible with respect to our implementation time. Secondly, we have neglected $SWCNT - SWCNT$ interaction [21] and $C_{60} - SWCNT$ interaction [22, 23], which are far from the resonance frequency of the electron spin under our consideration. In experiments, however, the $C_{60} - SWCNT$ interaction, although very weak, should be seriously considered, which would influence the transport of the mobile electron. Thirdly, no operational imperfection was involved in our treatment above. Actually any deviation from the desired time in switching off the potential well and in radiating the ESR pulse would yield additional phases and lower the fidelity. But a nearly perfect operation of our scheme seems challenging with current technology.

Besides the application mentioned in Fig. 1, our idea could also be generalized to entangling two or many spatially separated static qubits in the same $SWCNT$ (See Fig. 4) and to fusing two entangled states prepared respectively in two $SWCNTs$ [24]. As shown in Fig. 4(a), the output electron with different spin polarization from a $SWCNT$ goes in different ways due to the polarizing beam splitter, and then gets recorded by the charge detector. The Bell states of the two static qubits $|\Phi\rangle^+ = (|\downarrow\rangle |\downarrow\rangle + |\uparrow\rangle |\uparrow\rangle) / \sqrt{2}$ and $|\Phi\rangle^- = (|\downarrow\rangle |\downarrow\rangle - |\uparrow\rangle |\uparrow\rangle) / \sqrt{2}$ are thereby generated in the case of $P_e = 0$ and $P_e = 1$, respectively. Likewise, the GHZ state of n static qubits $|\text{GHZ}\rangle^\pm = (|\downarrow\rangle_1 |\downarrow\rangle_2 \cdots |\downarrow\rangle_n \pm |\uparrow\rangle_1 |\uparrow\rangle_2 \cdots |\uparrow\rangle_n) / \sqrt{2}$ could also be produced when $P_e = 0$ or $P_e = 1$ (See Fig. 4(b)). Comparing to a previous work with two electrons interacting and entangling in a $SWCNT$ [11], our scheme is relatively simpler. As the wavefunction of the static electron is completely compressed in the cage, there is no wavefunction overlap between the static and mobile electrons in our case. As a result, no concern about the quantum characteristic of two identical particles is needed in our case, and the entanglement between the mobile and static qubits could be deterministically achieved by magnetic dipole-dipole interaction.

In summary, we have proposed a potential scheme to entangle two electron spins in distant fullerene peapods. To accomplish our idea, we have to employ ESR selective pulses, magnetic field gradient, and $SWCNTs$ with switchable potential wells. Although some of the operations in our scheme are still unreachable with current techniques, we argue that our scheme would be helpful for achieving large-scale QIP setup with fullerene-based qubits.

This work is supported by NNSF of China under Grants No. 10774163 and No. 10774042.

-
- [1] V. Vedral, Nature (London) **453**, 1004 (2008); R. Blatt and D. Wineland, *ibid* **453**, 1008 (2008); I. Bloch, *ibid* **453**, 1016 (2008); H. J. Kimble, *ibid* **453**, 1023 (2008); J. Clarke and F. K. Wilhelm, *ibid* **453**, 1031 (2008).
 - [2] D. L. Moehring *et al.*, Nature (London) **449**, 68 (2007).
 - [3] W. Harneit, Phys. Rev. A **65**, 032322 (2002).
 - [4] D. Suter *et al.*, Phys. Rev. A **65**, 052309 (2002).
 - [5] J. Twamley, Phys. Rev. A **67**, 052318 (2003); J Twamley *et al.*, New J. Phys. **8**, 63 (2006); M. Feng and J. Twamley, Phys. Rev. A **70**, 030303(R) (2004); C. Ju *et al.*, Phys. Rev. A **75**, 012318 (2007); W. Scherer *et al.*, J. Chem. Phys. **128**, 052305 (2008).
 - [6] M. Feng and J. Twamley, Phys. Rev. A **70**, 032318 (2004).
 - [7] S. Iijima, Nature (London) **354**, 56 (1991).

- [8] M. Bockrath *et al.*, Nature (London) **397**, 598 (1999); Z. Yao *et al.*, Nature (London) **402**, 273 (1999).
- [9] C. Bena *et al.*, Phys. Rev. Lett. **89**, 037901 (2002).
- [10] B. W. Smith *et al.*, Nature (London) **396**, 323 (1998); N. Bendiab *et al.*, Phys. Rev. B **69**, 195415 (2004); S. Rols *et al.*, Phys. Rev. B **71**, 155411 (2005); D. J. Hornbaker *et al.*, Science **295**, 828 (2002).
- [11] D. Gunlycke *et al.*, J. Phys.: Condens. Matter **18**, S851 (2006).
- [12] C. W. J. Beenakker *et al.*, Phys. Rev. Lett. **93**, 020501 (2004).
- [13] X. L. Zhang, *et al.*, Phys. Rev. A **73**, 014301 (2006).
- [14] K. Tsukagoshi, *et al.*, Nature (London) **401**, 572 (1999).
- [15] J. W. G. Wildoer *et al.*, Nature (London) **391**, 59 (1998).
- [16] H. Chadli *et al.*, Phys. Rev. B **74**, 205412 (2006); A. Rochefort *et al.*, Phys. Rev. B **67**, 115401 (2003); M. -H. Du *et al.*, Phys. Rev. B **68**, 113402 (2003); P. Utoko, Appl. Phys. Lett. **89**, 233118 (2006); C. H. L. Quay, Phys. Rev. B **76**, 073404 (2007); L. Ge *et al.*, Phys. Rev. B **77**, 235416 (2008).
- [17] S. Tóth *et al.*, Phys. Rev. B **77**, 214409 (2008).
- [18] S. Knorr *et al.*, in *Electronic Properties of Novel Materials–Molecular Nanostructures*, edited by H. Kuzmany *et al.*, AIP Conf. Proc. No. 544 (AIP, Melville, NY, 2000), p. 191.
- [19] This simplified treatment is correct only under the assumption that the operation after the *CNOT* gating is very fast and thereby the generated dephasing is negligible with respect to the phase generated before the *CNOT* gating. A more strict study with master equation under the transport theory is underway.
- [20] The electronic conductivity of carbon nanotube depends heavily on the tube diameter and wrapping angle, with slight shift of which the carbon nanotube could change from metallic state to semiconducting onr. So we may cite experimental data from both the metallic case and the semiconducting case.
- [21] A. Popescu *et al.*, Phys. Rev. B **77**, 115443 (2008).
- [22] S. Okada *et al.*, Phys. Rev. Lett. **86**, 3835 (2001).
- [23] O. Dubay *et al.*, Phys. Rev. B **70**, 165424 (2004).
- [24] Consider a line of fullerenes confined in each peapod and the encapsulated electron spins have been entangled. Supposing that the two endohedral fullerenes plotted in Fig. 1 are the end ones of the fullerene lines, we would fuse the two lines of entangled electron spins in the peapods by entangling the mobile qubits by a Bell-state analyzer.

Captions of Figures

FIG. 1 Schematic setup to generate entanglement between two electron spins in two distant endohedral fullerene peapods in $x-y$ plane under magnetic field gradient B_Z . The static qubits A' and B' are caged in fullerenes inside the *SWCNTs*. The mobile qubits A and B are injected and bound in shallow potential wells, which could be switched on and off at will. The mobile qubits, after entangling with the static qubits by ESR pulses (denoted by wavy arrows), will be moved to the Bell-state analyzer in the dashed box (See Fig. 3(a) in [13]) where P_1 and P_2 are encoders which perform the spin parity measurement and record bunching ($P_1 = P_2 = 0$) and antibunching ($P_1 = P_2 = 1$). H means a Hadamard gate $H = (\sigma_x + \sigma_y)/\sqrt{2}$.

FIG. 2 The eigenenergy spectrum of the two electron spins coupled by the magnetic dipole-dipole interaction, where $|\cdot\rangle$ is the state consisting of a mobile and a static qubits, and $\{\cdot\}$ at the bottom and on the right represent, respectively, the degenerate frequency difference between the nearest-neighbor levels along a column and along a line.

FIG. 3 The fidelity of the Bell states $|\Psi\rangle_{A'B'}$ (bottom surface) and $|\Phi\rangle_{A'B'}$ (top surface) in a dissipative situation, where $K_1 = \Omega_e/\Gamma_1^A$ and $K_2 = \Omega_e/\Gamma_1^B$. The *CNOT* gating time we set is $t_g = \pi/\Omega_e$ with $\Omega_e = 25$ MHz. The inset shows the fidelity of the Bell states in the case of $K_1 = K_2 = K$, where the solid and the dashed curves represent the fidelity of the Bell states $|\Psi\rangle_{A'B'}$ and $|\Phi\rangle_{A'B'}$, respectively.

FIG. 4 The schematics for an application of our scheme, where the mobile qubit is initially prepared in a superposition state $(|\uparrow\rangle + |\downarrow\rangle)/\sqrt{2}$, and a line of endohedral fullerenes with static qubits prepared in $|\downarrow\rangle_1 |\downarrow\rangle_2 \cdots |\downarrow\rangle_n$ are confined in a *SWCNT*. By employing bias voltages and ESR pulses, in combination with the Hadamard gate, the charge detector P_e (counting the charge number 0, 1 and 2 [12]) and a polarizing beam splitter (denoted by double dashed lines) which transmits spin up and reflects spin down, we could create entanglement of the static qubits in a controllable way. (a) The creation of Bell states of two spatially separated static qubits; (b) The creation of GHZ states of n static qubits.

TABLE I. List of the resulting Bell states corresponding to different outputs from the encoders P_1 and P_2 . From [13], the entangled state of the mobile electrons A and B , input respectively from port a and b , could be $|\Psi\rangle_{AB}^\pm$ if $P_1 = 0$ or $|\Phi\rangle_{AB}^\pm$ if $P_1 = 1$. After the Hadamard gating, $P_2 = 1$ may correspond to $|\Psi\rangle_{AB}^+$ or $|\Phi\rangle_{AB}^+$ and $P_2 = 0$ means $|\Psi\rangle_{AB}^-$ or $|\Phi\rangle_{AB}^-$. Therefore, considering the detection results from P_1 and P_2 together, we could specify the entanglement between the mobile qubits A and B , which yields the entanglement between A' and B' by Eq. (3).

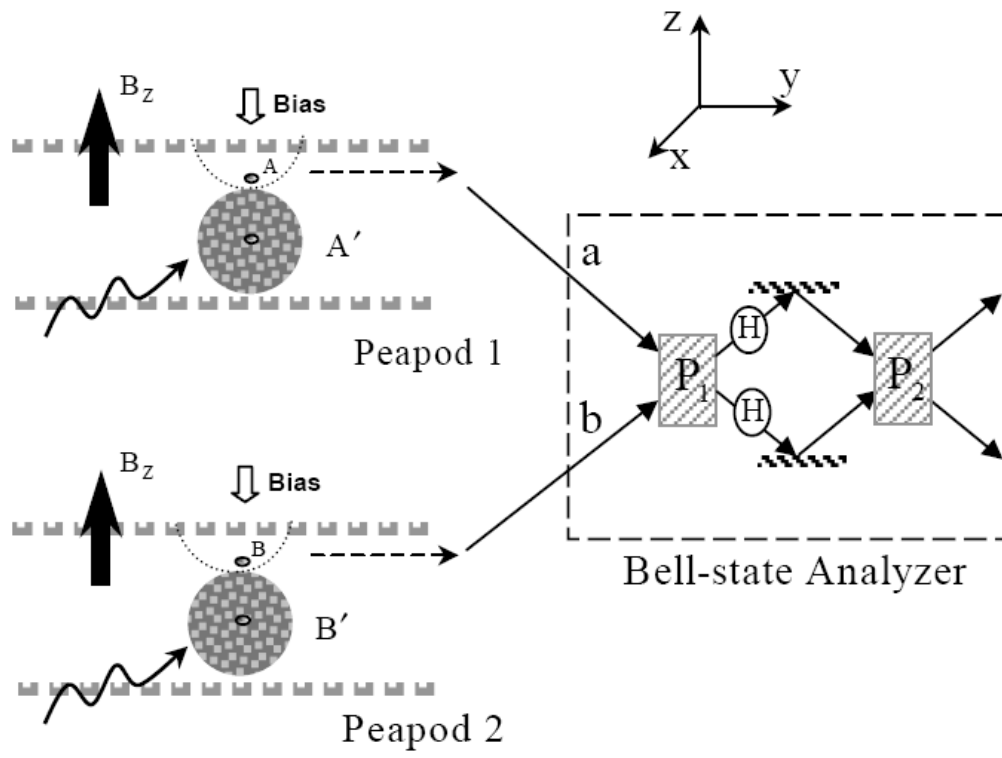
Outputs from encoders	$ \Psi\rangle_{AB}$	$ \Psi\rangle_{A'B'}$
$P_1 = 0; P_2 = 1$	$ \Psi\rangle_{AB}^+ = \frac{1}{\sqrt{2}}(\uparrow\rangle_A \downarrow\rangle_B + \downarrow\rangle_A \uparrow\rangle_B)$	$ \Psi\rangle_{A'B'}^+ = \frac{1}{\sqrt{2}}(\downarrow\rangle_{A'} \uparrow\rangle_{B'} + \uparrow\rangle_{A'} \downarrow\rangle_{B'})$
$P_1 = 0; P_2 = 0$	$ \Psi\rangle_{AB}^- = \frac{1}{\sqrt{2}}(\uparrow\rangle_A \downarrow\rangle_B - \downarrow\rangle_A \uparrow\rangle_B)$	$ \Psi\rangle_{A'B'}^- = \frac{1}{\sqrt{2}}(\downarrow\rangle_{A'} \uparrow\rangle_{B'} - \uparrow\rangle_{A'} \downarrow\rangle_{B'})$
$P_1 = 1; P_2 = 1$	$ \Phi\rangle_{AB}^+ = \frac{1}{\sqrt{2}}(\uparrow\rangle_A \uparrow\rangle_B + \downarrow\rangle_A \downarrow\rangle_B)$	$ \Phi\rangle_{A'B'}^+ = \frac{1}{\sqrt{2}}(\downarrow\rangle_{A'} \downarrow\rangle_{B'} + \uparrow\rangle_{A'} \uparrow\rangle_{B'})$
$P_1 = 1; P_2 = 0$	$ \Phi\rangle_{AB}^- = \frac{1}{\sqrt{2}}(\uparrow\rangle_A \uparrow\rangle_B - \downarrow\rangle_A \downarrow\rangle_B)$	$ \Phi\rangle_{A'B'}^- = \frac{1}{\sqrt{2}}(\downarrow\rangle_{A'} \downarrow\rangle_{B'} - \uparrow\rangle_{A'} \uparrow\rangle_{B'})$

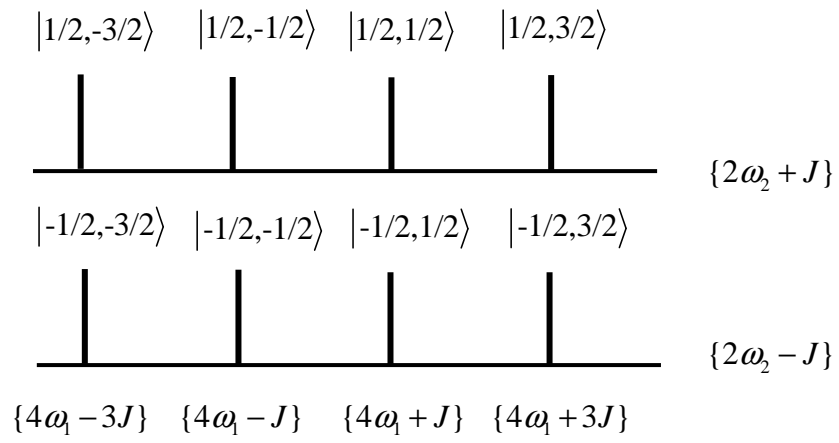
FIG. 1:

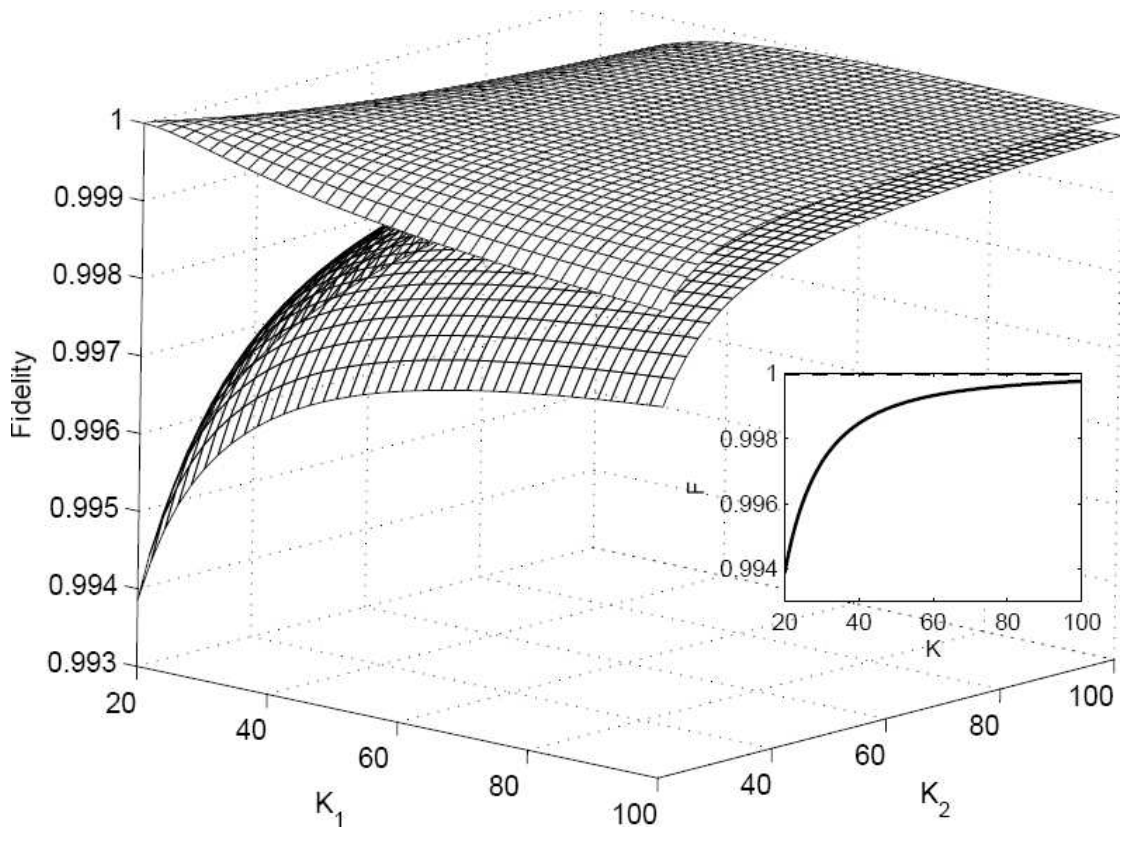
FIG. 2:

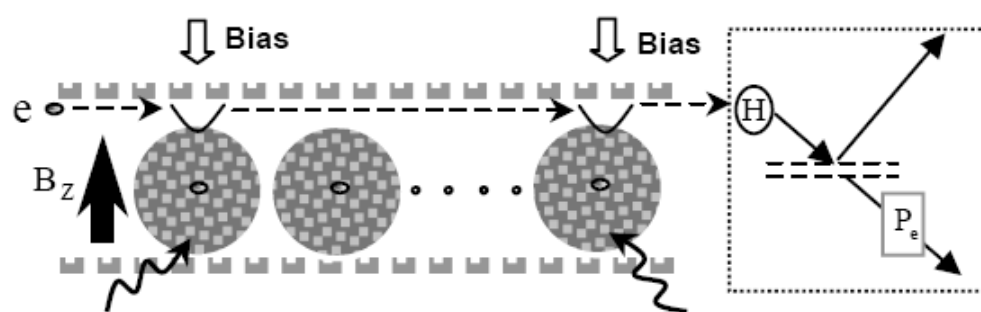
FIG. 3:

FIG. 4:

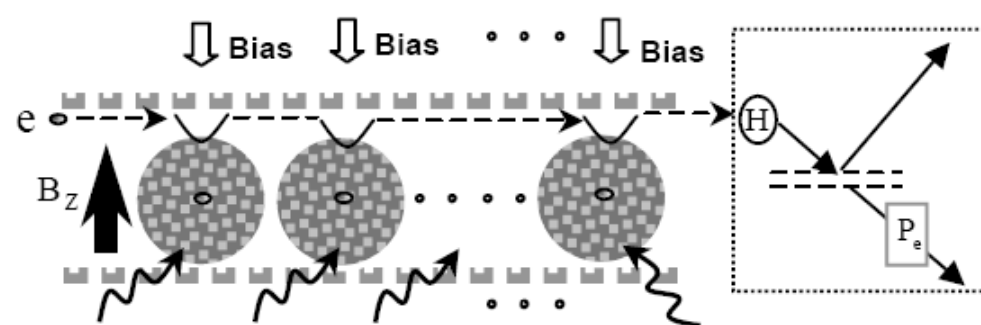








(a)



(b)